Research Article

Calculation of buckling loads of IPE-section bending members based on optimization of analytical formulations

Ahmet ÖZBAYRAK[1],* , Mohammed Kamal ALI[2] , Hatice ÇITAKOĞLU[1]

[1]Department of Civil Engineering, Faculty of Engineering, Erciyes University, Kayseri, 38039, Türkiye
[2]Department of Civil Engineering, College of Engineering, University of Kirkuk, Kirkuk, 36001, Iraq

ABSTRACT

The critical lateral buckling load of cantilever beams with IPE cross-section was calculated using analytical closed-form equations and numerical finite element analyses within the scope of the research. The equations suggested in the specifications for simply supported beams were used to calculate the buckling load of cantilever beams. The rationality of the values calculated due to this is not fully known. In the research, a single loading was made to the shear center at the free end of the cantilever beam. Cantilever length and section height were kept variable. As a result, it has been determined that there are partial differences in the analysis result obtained from the elastic stability theory and finite element method. Accordingly, the results obtained from ANSYS and SAP2000 analyses confirm each other. On the other hand, the results obtained using the formulation of Timoshenko and Gere, the calculation results made according to the AISC and DCCPSS regulations, and the results obtained from the LTBeam program confirm each other. However, it differs from the FEA analysis due to the cantilever beam length's shortening and the section height increase. Thus, to obtain accurate and reliable results in the buckling load calculation of cantilever beams, the equations used in analytical calculations were optimized according to finite element analysis (FEA) results. As a result of the study conducted according to the error criteria, it was determined that the updated equation results gave similar results to the FEA results.

Cite this article as: Özbayrak A, Ali MK, Çıtakoğlu H. Calculation of buckling loads of IPE-section bending members based on optimization of analytical formulation. Sigma J Eng Nat Sci 2024;42(4):973–987.

INTRODUCTION

In the lateral buckling calculations of steel beams, the design methods of simply supported and cantilever beams given in the regulation are the same. However, due to the different end support conditions in cantilever beams, the maximum displacement and buckling angle occur at the free ends instead of the middle of the span. The buckling modes obtained as a result of this situation are different from each other. Therefore, the recommended methods for simple support beams are not suitable for cantilever beams

*Corresponding author.
*E-mail address: ozbayrak@erciyes.edu.tr

[1]. AISC or DCCPSS regulations do not guide the lateral buckling of cantilever beams [2,3]. This research aims to provide rational information against lateral buckling in the design of steel cantilever beams. In general, the concepts of lateral buckling of beams and lateral-torsional buckling are explained in many books in the literature. Accordingly, the elastic lateral torsion buckling load under the bending effect of simple supported beams can be solved with the help of closed-form equations [4–7]. However, analytical solutions become very complex when beam end conditions differ from simple support. Therefore, numerical approximations such as the finite element method are needed to solve basic differential equilibrium equations [8–10]. The load-displacement relationships of I-section steel cantilevers were investigated by [11]. Under the effect of a single load at the free end, numerical and experimental results were compared. Accordingly, estimating the buckling load by numerical analysis with the ABAQUS program during the design phase was considered an acceptable method. Studies on unsymmetrical I-section cantilever beams were carried out by Samanta and Kumar [12]. In the studies, single load, distributed load, and moment were affected at the beam end. With the help of the ABAQUS program, the buckling load was investigated by giving lateral support to the top flange, bottom flange, and both. Accordingly, it has been found that if loading is made to the lower flange, the side support position does not significantly affect the cantilever beam buckling capacity. Özbaşaran et al. presented alternative design methods for calculating the buckling load and movement of I-section cantilever beams under the effect of lateral-torsional buckling [13]. In the critical elastic lateral-torsional buckling load calculation, the results of the closed-form equations, the analysis made by ABAQUS, and the experimental findings were found in accordance with the results of the proposed design method. Ma et al. conducted a study on elastic lateral buckling of unsymmetrical I-section cantilever beams [14]. According to the Rayleigh-Ritz method, while the profile flanges remain linear during buckling, it is assumed that the web part is susceptible to distortion. The accuracy of the proposed method has been verified with the help of the NASTRAN program, which calculates according to the finite element method. The elastic lateral torsional buckling behavior of tapered beams with different support conditions has been investigated by Andrade et al. [15]. A better understanding of the tapered beam behavior was provided by providing concrete explanations for some of the results regarded as illogical in the research. Zhang et al. conducted studies on the lateral-torsional buckling behavior of I-section cantilever beams with stiffening plates [16]. An analytical solution of the dimensionless buckling equation of these beams was obtained with the help of dimensionless parameters. The dimensionless critical moment formula developed with the help of mathematical optimization analysis software (1stOPT) has been verified with ADINA finite element software. A simple and useful calculation method for practical engineering

calculations is presented in the research. The results of the finite element analysis of the elastic lateral-torsional buckling strength of light steel cantilever beams under the effect of transverse loading were shared by Kurniawan and Mahendran [17]. Accordingly, the applicability of modification factors in various steel design codes was reviewed, and the design approach in the AS4100 code was proposed for light steel cantilever beams subjected to transverse loading. The study carried out by Trahair stated that the lateral buckling formulations suggested in the design regulations for simply supported beams with uniformly distributed loads are not suitable for cantilever beams [7]. His study aimed to develop simple approximate methods in the design of cantilever beams against inelastic lateral buckling. Within the scope of the research conducted by Yılmaz and Kıraç [18], an equation that can be used to calculate the critical torsional buckling load of the IPE and IPN simple support beams in European norms was presented [18]. The slenderness of the profile section and the effect of loading positions were taken into account in their study. Consistent results were obtained among analytical, parametric, and numerical solutions. It has been found that the lateral torsional buckling load of European IPE and IPN beams can be determined by the presented equation and used safely in design procedures. I-section composite beams are discussed by Prombut and Anakpotchanakul [19]. It has been observed that the bending results obtained from the shear deformation theory and finite element analysis in beams under uniformly distributed load applied to the upper flange are compatible with each other. It is stated that thanks to the validated finite element procedure, realistic results can be obtained based on curvature, taper, and buckling along the length of an I-section. Özbaşaran and Yılmaz introduced shape optimization for symmetrical I-section beams with tapered flanges and/or web [20]. The optimization procedure was created using the Big Bang - Big Crunch algorithm and Deb's constraint handling method. The designs made were verified by finite element analysis. It has been shown that tapering in absolute conditions may not significantly affect the material economy. Trahair stated that the design methods given in regulations such as AS4100, BS595, Eurocode3, and AISC for lateral buckling of cantilever beams are modifications of the rules introduced according to simple support beams [1]. The accuracy of these modifications was found to be questionable, and it was emphasized that they could not fully guide the design. A different method has been developed, and the solution has been summarized with examples.

Minimizing the cost and weight of products has been an area of interest for many industries. It is among these sectors in reinforced concrete and steel structures. Complex situations arise in reinforced concrete and steel structures design due to the nonlinear structure behavior and related design equations. In addition, the behavior of the designed sections under the effect of dynamic loads also creates complex situations. These problems are sizing optimization

problems [21]. Previous optimization studies on reinforced concrete and steel structures are based on weight and cost [22–30]. Shaqfa and Orbán improved the position of the upper and lower flexural member, simultaneously minimizing cost, weight, and cost-weight [31]. Hayalioğlu and Değertekin presented a genetic algorithm for designing the optimum cost of nonlinear steel frames with semi-rigid connections subject to the displacement and stress restrictions of the American Institute of Steel Construction-Allowable Stress Design (AISC-ASD) regulation [23]. As a result of their studies, they stated that more economical optimum frames could be obtained by adjusting the stiffness of the connections in frame systems. Omkar et al. used Particle Swarm Optimization (PSO) to minimize the weight and total cost of the composite component to achieve a certain strength of composite components [32]. Barraza et al. used Genetic Algorithm (GA) and Particle Swarm Optimization (PSO) to minimize the structural weight of steel structures exposed to earthquake loads and to improve the structural performance of buildings [33]. As a result of their studies, they emphasized that they generally obtained better solutions with PSO in structural buildings compared to the GA approach. Another issue of sizing optimization is to maximize the cross-section against torsion and fracture [34–37]. Cho optimized the design of a composite cylindrical shell against buckling and fracture and stated that the optimized composite cylindrical shell exhibits significantly improved mechanical properties compared to the traditional design as result of the study [36]. Many optimization studies are also done in Excel–Solver [37–39]. Taki optimized the dimensions of the Z-hardened panel under compression load with Excel-solver to update Farrar's work. As a result of the work, he developed design charts for Z-hardened panels and produced a design guide [40]. Msabawy and Mohammad used the Generalized Reduced Gradient (GRG) algorithm in the Solver Add-on tool in Microsoft Excel to perform first-order elastic structural analysis of semi-rigid steel portal frames [37]. Msabawy and Mohammad used the GRG algorithm to optimize cross-sectional areas in cold-formed steel frames [39]. As a result of their studies, they stated that it proved the reliability and validity of the GRG algorithm in terms of the ability to obtain optimum configurations of optimized sections. In addition to the sizing optimization problem in reinforced concrete and steel structures, there are modification studies of theoretical equations. Perelmuter and Yurchenko determined the optimum height and weight of the tower by changing various equations depending on the capacity of the wind-powered generator's generated energy [30]. Based on the concepts of the Euler-Bernouli beam theory and fracture mechanics, Vosoughi reformulated the management equation using genetic algorithms (GA) and particle swarm optimization (PSO) techniques [41]. They showed the convergence, efficiency, and accuracy of the optimization method with the finite element method by solving different examples. Le et al. took into account the Adaptive Neuro-Fuzzy Inference System (ANFIS) using the

GA and PSO to assess the buckling damage of steel columns subjected to axially compressive load [42]. They concluded that the ANFIS-PSO method significantly outperformed the ANFIS-GA method with a correlation factor of 0.929. Jung et al. working to assess the tensile characteristics of high strength steel, used Artificial Neural Networks (ANN) and back-propagated linear regression [43]. They asserted that using a deep learning system produced predictions of yield strength, yield ratio, and tensile strength with high accuracy. Cuong-Le et al. introduced a PSO-optimized Support Vector Machine (SVM) to identify deterioration in truss and frame constructions [44]. Additionally, they contrasted the suggested approach with ANN, Deep Neural Networks (DNN), and Adaptive Neuro-Fuzzy Inference System (ANFIS). They concluded that the damage and the degree of damage for truss and frame structures were successfully identified using the proposed strategy, outperforming the other techniques. Das and Das have used Random Forest Regressor (RFR) to evaluate the fundamental natural frequencies of isotropic plate structures [45]. They have been considered as square, rectangular, thin, and thick plates whose materials have been selected as Structural Steel, Aernet 100, Al 7108, and Al 2024 for the isotropic plates. They claimed that the suggested strategy accurately predicts the fundamental natural frequency and is an adequate model for such a scenario. Özbayrak et al. conducted buckling load calculations using ANSYS on European I-section cantilever beams reinforced with transverse stiffener plates at various intervals [46]. They have created formulations employing multiple linear regression analysis and multigene genetic programming techniques to estimate the found load values more effectively. According to their statement, the lateral buckling stress according to the transverse stiffener plate spacing for European I-section cantilever steel beams can be calculated with formulations created using computer technology.

In the construction literature, more studies use machine-learning models of steel I-beams and cantilever beams. Artificial intelligence has enabled the suggested formula to successfully forecast the residual lateral buckling capacity of steel I-beams, according to research on artificial neural networks [47]. In a different study, a deep learning classifier was used to determine the damage status of cantilever beams in an invasive-free manner with the maximum level of accuracy [48]. Artificial neural networks were used to assess the twisting performance of a steel I beam that was externally attached to sheets with polymer matrix reinforcement enhanced with various fibers to reduce the experimental work [49]. Additionally, the web-post buckling shear strength of cellular beams and the load-bearing capability of castellated steel beams were predicted using artificial neural network models [50,51]. Thanks to a database provided by a study that included 475 finite element models, the lateral torsional buckling strength was calculated using an artificial neural network and the multiple regression approach [52]. An adaptive neuro-fuzzy

inference system was used to develop empirical equations for estimating natural frequencies from a finite element dataset [53]. Additionally, form optimization makes use of artificial intelligence. Using a genetic algorithm, the stiffness of cold-formed steel sections was increased [54].

Within the scope of the research, analytical calculations were compared with the results of numerical analysis. It has been observed that the calculations made with the LTBeam program are compatible with the analytical calculation results. Critical lateral buckling loads found from analytical equations and LTBeam program results are consistent in this regard. However, it has been determined that there are some differences between these and the FEA results depending on the profile cross-section and length. In the studies in the literature, it is stated that the analysis made according to the finite element method with the help of developing computer technology is more accurate than the calculations made with closed-form equations. First, using two different FEA programs, lateral buckling loads calculated in the ANSYS program were verified with the help of the SAP2000 program. Later, studies were carried out to harmonize the results from the equations given in Timoshenko, Gere, and other Regulations with FEA results (ANSYS). Using optimization techniques, the equation given by Timoshenko and Gere and formulations given in AISC and DCCPSS regulations were successfully updated.

MATERIALS AND METHODS

In the case of a single load acting on the shear centre at the free end of the IPE section cantilever beam, the lateral

buckling load was calculated and compared with five different methods. These are, respectively, elastic stability theory, regulation on design, calculation, and construction principles of steel structures (DCCPSS), LTBeam program, SAP2000, and ANSYS software (Figure 1). In the calculations, the material elasticity modulus was 210000 MPa, the shear modulus was 80769 MPa, and the Poisson ratio was 0.3. The section heights of the cantilever beams used in the study include all IPE profiles in the range of 100-600 mm. Cantilever beam lengths were evaluated in five different sizes: 1000 mm, 1500 mm, 2000 mm, 2500 mm, and 3000 mm.

Calculation According to Elastic Stability Theory

The critical value of the lateral buckling load for cantilever beams is calculated as given in Equation 1 by Timoshenko and Gere [6], depending on the boundary conditions of the beam endpoints.

$$P_{cr} = \gamma_2 \frac{\sqrt{E \cdot I_y \cdot C}}{L^2} \qquad (1)$$

The factor γ_2 in this expression is a dimensionless coefficient obtained according to the ratio L^2C/C_1. The values of this coefficient are as given in Table 1.

As the L^2C/C_1 ratio increases, the γ_2 factor approaches the 4.013 limit value. This value corresponds to the critical load of thin rectangular beams. If ratio L^2C/C_1 takes values greater than 40, the approximate factor γ_2 is calculated as given in Equation 2.
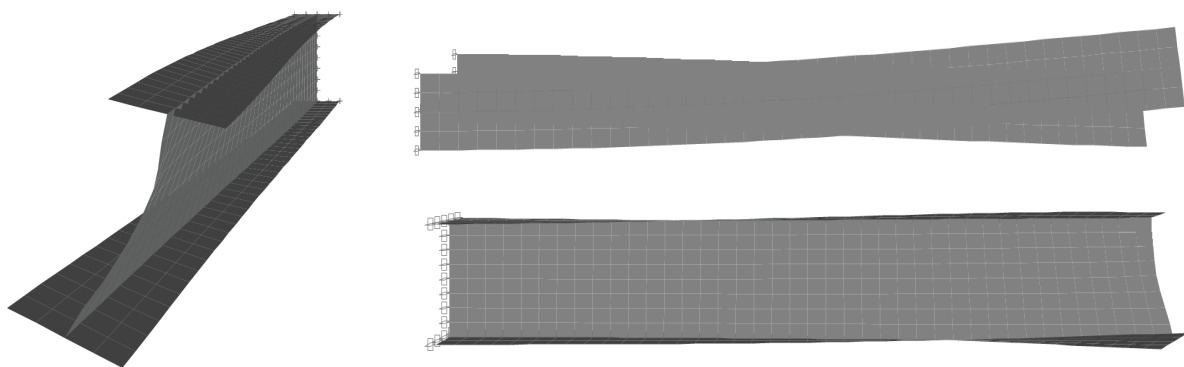

Figure 1. Lateral-torsional buckling condition.

Table 1. Factor γ_2 for I-section cantilever beams

L^2C/C_1	0.1	1	2	3	4	6	8
γ_2	44.3	15.7	12.2	10.7	9.76	8.69	8.03
L^2C/C_1	10	12	14	16	24	32	40
γ_2	7.58	7.20	6.96	6.73	6.19	5.87	5.64

$$\gamma_2 = \frac{4.013}{(1 - \sqrt{C_1/L^2 C})^2} \tag{2}$$

Calculation According to AISC and DCCPSS Regulations

In the case of lateral torsion buckling boundaries, the positive contribution of the bending moment distribution along the length between the points supported by the lateral stability connection is taken into account by the coefficient given in Equation 3. The regulations stipulate that this coefficient in cantilever beams is taken as $C_b = 1$ with an approach on the safe side. However, since it was determined that this approach has a limited contribution, the expression given in Equation 3 was used within the scope of the research.

$$C_b = \frac{12.5 M_{maks}}{2.5 M_{maks} + 3 M_A + 4 M_B + 3 M_C} \tag{3}$$

The critical stress value of I-cross section elements with double symmetry axes, whose web and flange parts are compact and under the effect of bending around their strong principal axes, are calculated with the expression given in Equation 4 according to the lateral-torsional buckling.

$$F_{cr} = \frac{C_b \cdot \pi^2 \cdot E}{(L_b/i_{ts})^2} \sqrt{1 + 0.078 \frac{J \cdot c}{W_{ex} \cdot h_o} \left(\frac{L_b}{i_{ts}}\right)^2} \tag{4}$$

The effective radius of inertia used in the critical stress value formulation is as given in Equation 5.

$$i_{ts}^2 = \frac{\sqrt{I_y \cdot C_w}}{W_{ex}} \tag{5}$$

Accordingly, the critical value of the lateral-torsional buckling load of the I cross-section elements under the bending effect is calculated as given in Equation 6 in the regulations.

$$P_{cr} = \frac{F_{cr} \cdot W_{ex}}{L_b} \tag{6}$$

Calculation According to Finite Element Method

Finite element models of beams were created with the help of ANSYS, SAP2000 and LTBeam software. Critical lateral buckling load analysis was performed with the help of the created models. Accordingly, three-dimensional solid modelling of cantilever beams was created in the analysis made with ANSYS software (Figure 2) The material type of the created models was defined as SOLID187. In the analysis made according to linear elastic material properties, cantilever beams were divided into finite elements with an average range of 2.5 ~ 5 cm. Fixed support was defined at the nodal point on one side of the beam endpoints, and a 1 N unit loading was made to the shear centre on the other free end. The analysis type was selected as Eigen Buckling and the value calculated as buckling load factor at the end of the analysis gave the buckling load.

According to the analysis made by utilizing the SAP2000, the cantilever beam body and flange elements are defined using the Shell Element. (Figure 3). In the models, flange and web joints were combined at 90° angles. Cantilever beams with linear elastic material properties were divided into finite elements with an average range of 2.5 ~ 5 cm. Fixed support properties were assigned to the nodes on one side of the beam endpoints. The shear centre at the other free end was loaded with 1 N unit loading. P-Delta effects were taken into consideration by selecting the analysis type

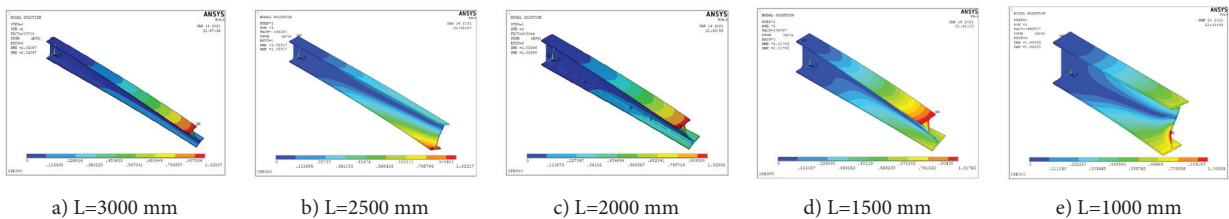a) L=3000 mm   b) L=2500 mm   c) L=2000 mm   d) L=1500 mm   e) L=1000 mm

Figure. 2. Cantilever beams modelled in ANSYS program.

a) L=3000 mm   b) L=2500 mm   c) L=2000 mm   d) L=1500 mm   e) L=1000 mm
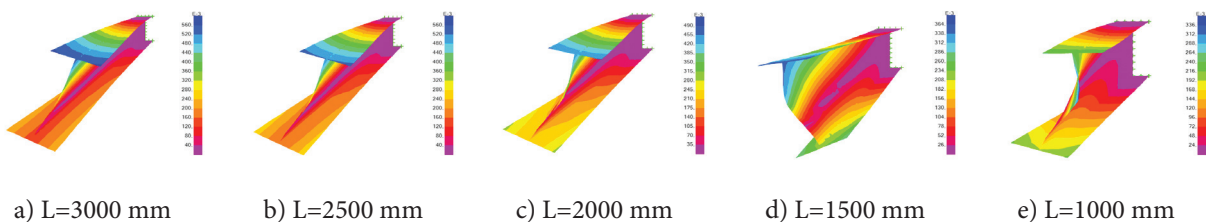
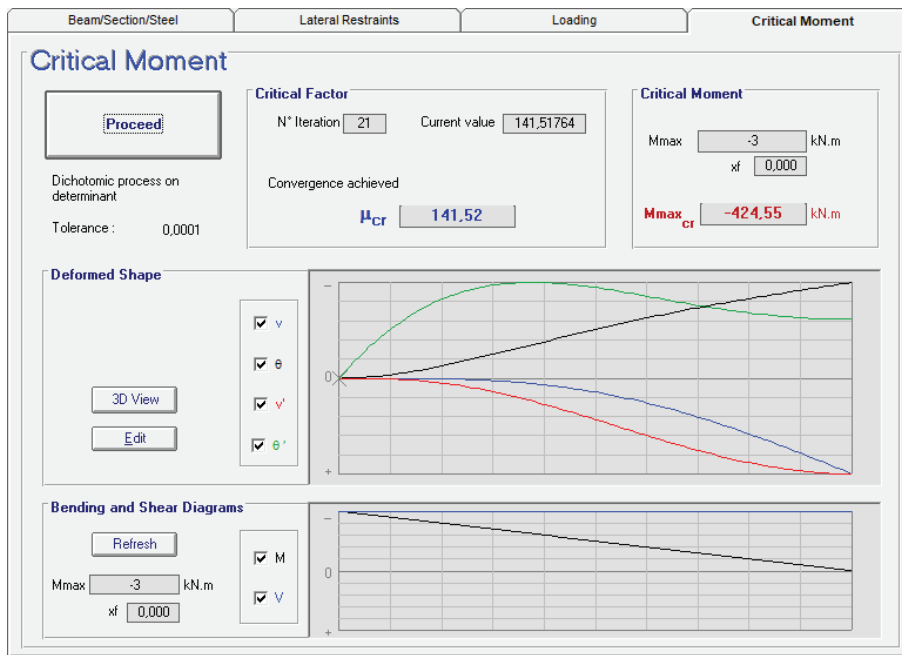**Figure 3.** Cantilever beams modelled in the SAP2000 program.

Figure 4. Cantilever beams modelled in LTBeam program.

as Buckling. As a result of the analysis, the value obtained as the buckling load factor gives the buckling load value.

LTBeam is free software developed by CTICM (Center Technique Industriel de la Construction Métallique) in France, used only for the calculation of critical moments [55]. Critical elastic lateral-torsional buckling loads can also be determined through one-dimensional finite element models, where beams are modeled according to their actual geometry using LTBeam software. (Figure 4).

The program can perform buckling analysis of both simply supported beams and cantilever beams. Limited documentation on LTBeam made interpretation of results difficult. However, several reliable sources Access Steel (2005) and ECCS (2006) refer to LTBeam as a useful program [56,57].

Optimization With Microsoft Excel Solver

Solver is the simplest and most understandable computer software used to find the optimal result. Solver is an add-in command available in Microsoft Excel. Although it is a command included in Excel, the user must enable this command. Solver is used to find the largest or smallest value of the target cell in a formula. Constraints can be developed to the values to be used in models to be developed with the Solver and these restrictions can be applied to cells [Excel - help]. Using the lateral buckling load values of the IPE profile obtained from ANSYS program with the help of Excel Solver;

- The factor γ_2 in Equation 1 given by Timoshenko and Gere was calibrated [6].
- Fixed coefficients in Equation 4 given in AISC and DCCPSS regulations were calibrated.

The steps taken for calibration were listed below.

1. The Solver command is opened from the Data tab.
2. The target cell is determined by choosing one of values such as mean absolute error (MAE), root mean square error (RMSE), and mean absolute relative error (MARE).
3. The Largest is chosen if the target cell value is desired to be as large as possible, and the Smallest is chosen if it is desired to be as small as possible. If certain value is desired to be obtained, the value option is selected, and its value is written in the box. Since the error rate was desired to be the least in the study, the smallest option and RMSE value were chosen.
4. A variable cell must be determined for each coefficient in the equations to be calibrated. Each variable cell must have a direct or indirect relationship with the target cell. In the study, cells containing the values of coefficients a, b and c were selected as variable cells. Before starting the optimization process, a random number must be defined to the coefficients a, b and c.
5. Solver is based on Nonlinear Generalized Restricted Gradient (GRG), Simple LP and expansion methods. The nonlinear Generalized Restricted Gradient (GRG) method was used in the study.
6. After clicking the Solve command, the equation was solved by the data solver and the expansion coefficients that give the smallest error value were calculated.

Error Criteria

Error criteria were used to test the accuracy of the calibrated equations for the estimation of the lateral buckling load values of the IPE profiles. Commonly used error

criteria in the literature are Mean Absolute Relative Error (MARE), mean absolute error (MAE), mean square error (MSE), root mean square error (RMSE), determination coefficient (R^2) [58,59]. In this study, MARE, MAE, MSE, RMSE and R^2 error criteria were used. The fact that MARE, MAE, MSE and RMSE values are closest to zero and R^2 value is closest to one reflects the accuracy and power of the prediction. In addition, the Nash-Sutcliffe efficiency coefficient (NSE), proposed by Nash and Sutcliffe [60], has been used in many studies to measure estimation accuracy. The variance of the estimated data compared to the variance of the observed data is a normalized statistic that determines the relative size. NSE expresses to what extent the observed and predicted data converge [60]. MARE, MAE, MSE, RMSE and NSE values were calculated from the formulas given in Equation 7-11.

$$MARE = 100 \cdot \left(\frac{1}{n} \sum_{i=1}^{n} \left| \frac{BL_{p,i} - BL_{ansys,i}}{BL_{ansys,i}} \right| \right) \quad (7)$$

$$MAE = \frac{1}{n} \sum_{i=1}^{n} \left| BL_{p,i} - BL_{ansys,i} \right| \quad (8)$$

$$MSE = \frac{1}{n} \sum_{i=1}^{n} \left(BL_{p,i} - BL_{ansys,i} \right)^2 \quad (9)$$

$$RMSE = \frac{1}{n} \sum_{i=1}^{n} \sqrt{\left(BL_{p,i} - BL_{ansys,i} \right)^2} \quad (10)$$

$$NSE = 1 - \frac{\sum_{i=1}^{n} \left(BL_{p,i} - BL_{ansys,i} \right)^2}{\sum_{i=1}^{n} \left(BL_{ansys,i} - \overline{BL_{ansys}} \right)^2} \quad (11)$$

RESULTS AND DISCUSSION

Analytical and Numerical Findings

The critical lateral buckling load of I-section cantilever beams was calculated using a total of five different methods. The calculated buckling loads were obtained by applying a single load to the centre of shear at the free end of the beam. Although there are differences when the profile section increases and cantilever length decreases, the buckling load values calculated using the closed form equations and LTBeam program are close to each other. On the other hand, when the profile section is reduced and the cantilever length is increased, differences occur in the FEA results. However, the buckling load values calculated with the help of FEA generally confirmed each other. As a result, the results of the first three methods and the last two methods given in Table 2 are quite different from each other. This can be clearly seen in Figure 5.

Table 2. Lateral buckling load values calculated with different methods

Profile Type	Beam Length (mm)	Timoshenko (kN)	AISC- DCCPSS (kN)	LTBeam (kN)	ANSYS (kN)	SAP2000 (kN)
IPE 100	**1000**	40.18	39.36	40.44	37.44	11.23
IPE 120		74.03	71.94	73.83	69.76	35.05
IPE 140		127.87	125.38	126.77	113.22	66.57
IPE 160		209.12	208.97	207.47	121.78	98.05
IPE 180		329.12	334.59	324.40	194.45	132.95
IPE 200		497.23	516.59	493.53	203.16	170.85
IPE 220		777.32	800.37	749.76	297.87	219.68
IPE 240		1147.63	1197.99	1110.30	319.21	273.74
IPE 270		2146.85	1961.40	1771.40	479.70	353.49
IPE 300		4032.70	3103.90	2755.10	492.58	459.98
IPE 330		5881.12	4446.00	3923.00	676.51	557.10
IPE 360		8524.97	6392.55	5608.20	732.06	688.53
IPE 400		11748.40	8958.72	7819.20	854.77	832.07
IPE 450		16266.63	12778.91	11093.00	1070.22	1029.68
IPE 500		22154.84	18114.12	15656.00	1279.80	1254.17
IPE 550		29518.50	24797.49	21391.00	1551.16	1479.64
IPE 600		39465.72	34300.18	29512.00	1974.66	1830.02

Table 2. Lateral buckling load values calculated with different methods (*continued*)

Profile Type	Beam Length (mm)	Timoshenko (kN)	AISC- DCCPSS (kN)	LTBeam (kN)	ANSYS (kN)	SAP2000 (kN)
IPE 100	**1500**	15.09	15.26	15.12	14.96	0.93
IPE 120		26.78	26.45	26.95	26.04	4.20
IPE 140		45.22	44.05	45.43	41.66	14.30
IPE 160		73.31	71.32	73.39	62.39	33.28
IPE 180		113.51	110.87	112.95	85.32	59.11
IPE 200		171.76	168.80	170.06	114.40	86.15
IPE 220		256.21	256.34	254.27	146.67	119.08
IPE 240		375.37	380.28	372.89	189.23	153.26
IPE 270		586.02	609.80	580.41	234.77	200.59
IPE 300		916.78	952.75	884.95	296.73	263.50
IPE 330		1287.18	1359.60	1251.80	366.42	324.36
IPE 360		1784.93	1945.82	1775.40	452.60	410.13
IPE 400		2835.20	2718.34	2458.80	556.62	506.80
IPE 450		4704.91	3860.99	3457.90	692.70	644.73
IPE 500		7111.55	5457.19	4850.20	861.62	814.93
IPE 550		9850.19	7460.46	6604.60	1076.95	985.93
IPE 600		13685.47	10302.54	9079.00	1330.55	1273.27
IPE 100	**2000**	7.68	8.10	7.71	8.48	0.15
IPE 120		13.44	13.63	13.47	13.46	0.68
IPE 140		22.29	22.02	22.38	21.88	2.55
IPE 160		35.55	34.89	35.83	34.14	7.62
IPE 180		54.40	52.93	54.61	49.01	19.25
IPE 200		81.83	79.58	81.76	69.19	37.20
IPE 220		121.28	118.55	121.17	93.14	62.89
IPE 240		178.48	174.29	176.73	125.52	90.56
IPE 270		273.25	273.28	270.66	157.69	127.37
IPE 300		413.59	420.70	406.92	203.64	172.04
IPE 330		579.28	597.66	572.20	250.62	215.13
IPE 360		821.91	850.50	806.09	315.28	275.33
IPE 400		1148.93	1183.51	1110.20	383.08	341.32
IPE 450		1596.85	1671.94	1548.30	501.56	435.68
IPE 500		2190.69	2354.40	2158.40	623.86	554.99
IPE 550		2930.69	3212.96	2928.90	756.28	678.74
IPE 600		4677.88	4427.48	4010.90	940.96	882.53
IPE 100	**2500**	4.62	5.04	4.64	4.66	0.04
IPE 120		5.01	8.32	7.98	8.06	0.16
IPE 140		13.03	13.20	13.09	13.14	0.61
IPE 160		20.70	20.60	20.79	20.36	1.90
IPE 180		31.10	30.68	31.44	30.21	5.34
IPE 200		46.58	45.66	46.85	43.58	12.55
IPE 220		68.88	66.93	69.00	60.83	27.17
IPE 240		100.34	97.60	100.30	83.97	47.49
IPE 270		153.44	149.81	152.05	111.37	78.71
IPE 300		227.62	227.15	226.39	145.40	115.46
IPE 330		320.72	321.15	317.08	183.84	150.84
IPE 360		448.53	454.21	444.46	230.65	198.14
IPE 400		619.07	629.30	609.04	287.02	248.05
IPE 450		847.93	883.59	843.75	357.03	318.18
IPE 500		1204.29	1238.94	1170.30	446.34	407.00
IPE 550		1637.31	1687.23	1583.30	562.43	500.25
IPE 600		2235.76	2319.16	2160.30	703.94	650.52

Table 2. Lateral buckling load values calculated with different methods (*continued*)

Profile Type	Beam Length (mm)	Timoshenko (kN)	AISC- DCCPSS (kN)	LTBeam (kN)	ANSYS (kN)	SAP2000 (kN)
IPE 100	3000	3.08	3.44	3.08	3.11	0.01
IPE 120		3.29	5.62	5.25	5.32	0.05
IPE 140		3.54	8.81	8.53	8.49	0.19
IPE 160		13.37	13.61	13.44	13.88	0.59
IPE 180		20.06	20.00	20.18	19.94	1.69
IPE 200		29.90	29.54	29.96	28.98	4.18
IPE 220		43.54	42.73	43.88	41.22	10.21
IPE 240		63.10	61.89	63.59	59.46	21.10
IPE 270		95.81	93.21	95.68	80.80	43.34
IPE 300		142.61	139.31	141.52	107.71	73.51
IPE 330		200.10	196.04	197.65	139.41	104.75
IPE 360		276.97	275.53	276.06	186.65	145.01
IPE 400		380.57	380.04	376.98	222.18	186.48
IPE 450		524.17	530.18	519.59	287.56	242.90
IPE 500		727.46	739.97	717.59	348.59	313.45
IPE 550		979.80	1005.44	968.32	452.78	387.04
IPE 600		1319.75	1378.19	1317.40	551.96	504.52

The existing analytical method formulations have been optimized according to the FEA analysis results obtained by utilizing the ANSYS program. There are two main reasons for choosing the buckling load values to be referenced in FEA calculations from the ANSYS program instead of SAP2000. Firstly, cantilever beams are modelled as Solid elements in the ANSYS program and as Shell elements in SAP2000. Secondly, in SAP2000, while the web and flanges are joined perpendicular to each other at an angle of 90°; The web and flange joints of the models in ANSYS are curvilinear and exactly the same as the real profile geometry. For these reasons, the ANSYS program was used for the buckling load values taken as a reference within the scope of the research. The comparisons of the buckling load values of the IPE series cantilever beams of five different lengths calculated by five different methods are as given in Figure 5.

Optimization Technique Findings with Microsoft Excel Solver

In the second stage of the study, the a and b coefficients in Equation 12 were calibrated with the help of Excel–Solver, keeping the relationship between the γ_2 factor and the L^2C/C_1 ratio. The analyses have been conducted on a computer with an AMD Ryzen 7 PRO 3700 8-Core 3.60 GHz processor and 8 GB RAM. In addition, the c, d and f coefficients in Equation 13 of AISC and DCCPSS Regulations were calibrated with the help of Excel–Solver. At this stage, two different calibration processes were carried out using two different equations. The graph of the relationship between the ratio L^2C/C_1 given in Table 1 and γ_2 is given in Figure

6. As can be seen in Figure 6, there is an exponential relationship between the ratio L^2C/C_1 and γ_2 as in Equation 12. Therefore, the coefficients of Equation 12 were optimized to determine the γ_2 factor. In the advancing age of science, there are new methods for calculating lateral buckling load values as well as the Timoshenko and Gere [6] equation. The c, d and f coefficients of Equation 13 were calibrated by adhering to AISC and DCCPSS Regulations and using the lateral buckling load values obtained from the ANSYS program.

$$\gamma_2 = a \cdot \left(L^2 \cdot \frac{C}{C_1} \right)^b \tag{12}$$

$$F_{cr} = \frac{C_b \cdot \pi^2 \cdot E}{\left(\frac{L_b}{i_{ts}} \right)^2} \left(c + d \cdot \frac{J_c}{W_{ex} \cdot h_o} \cdot \left(\frac{L_b}{i_{ts}} \right)^2 \right)^f \tag{13}$$

c= 1, d= 0.078, f= 0.5

The coefficients of Equation 12 and Equation 13 were calibrated using Excel Solver so that the RMSE error criterion was the smallest. The coefficients of the calibrated equations are given in Table 3. As seen in Table 3, the new coefficients are different from each other. Comparison criteria for two different calibrated equations are given in Table 4. The approximate MSE values of the calibrated equations were obtained as 890, MARE values of 50 and
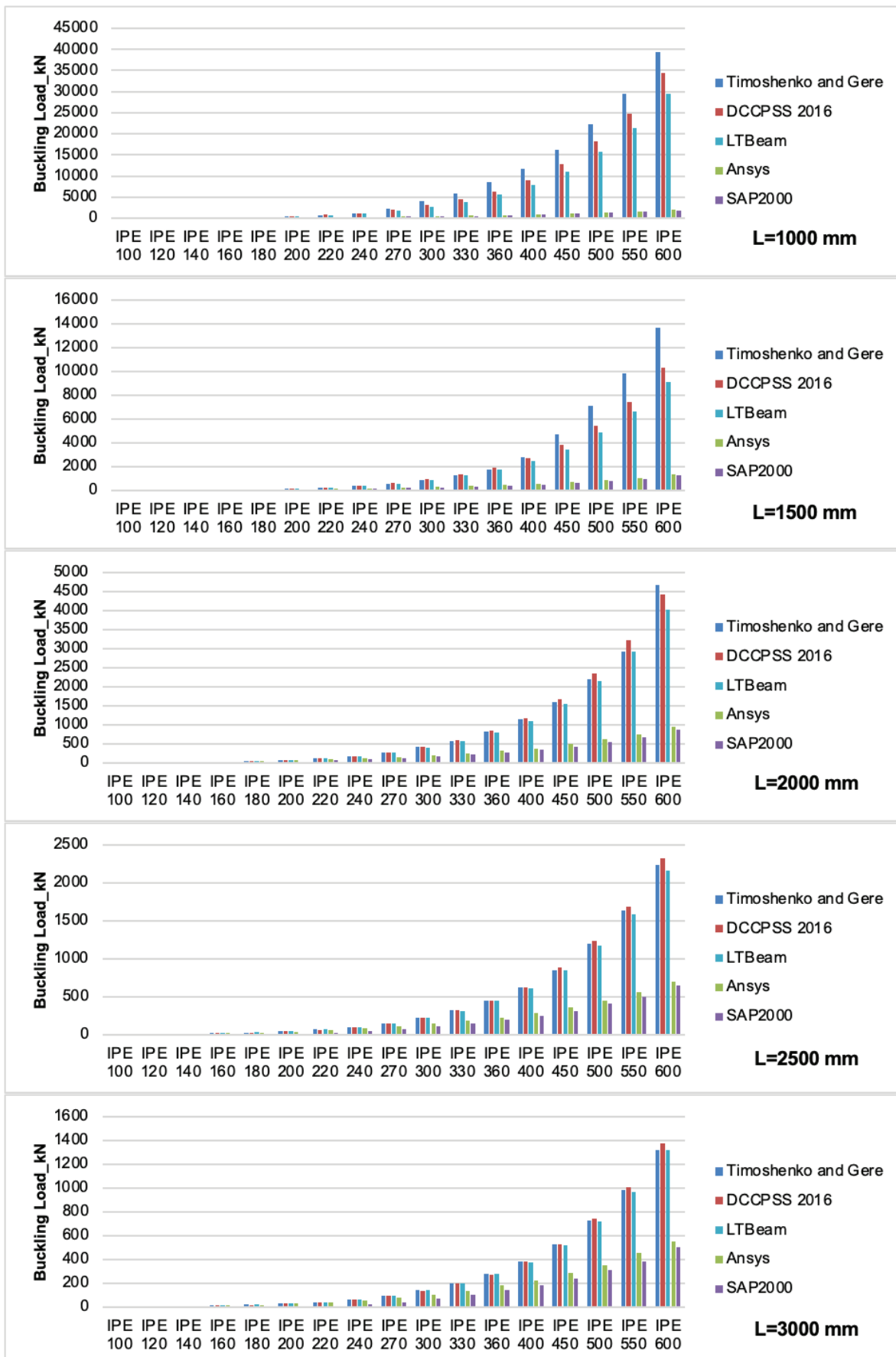
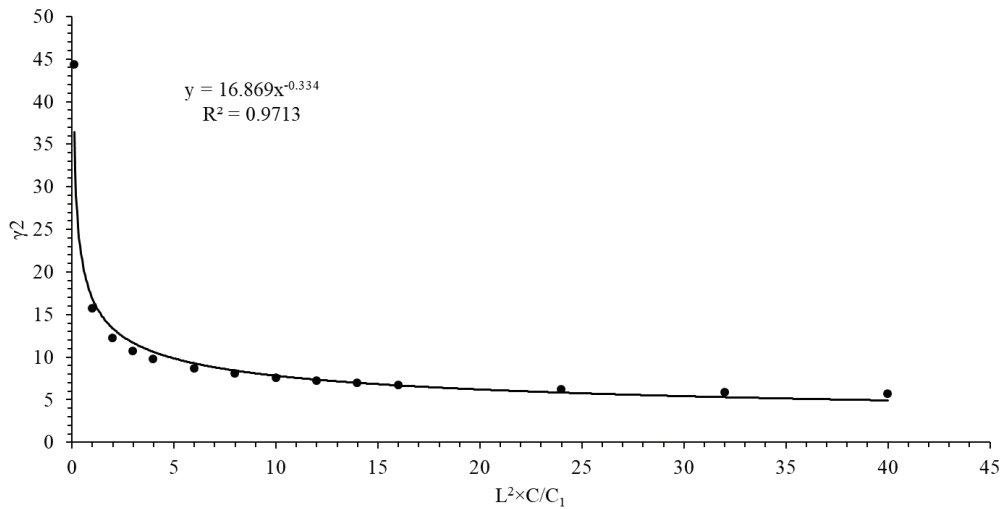**Figure 5.** Lateral buckling loads of cantilever beams of different lengths.

Figure 6. Relationship between L^2C/C_1 ratio and γ2

Table 3. Coefficients for calibrated models

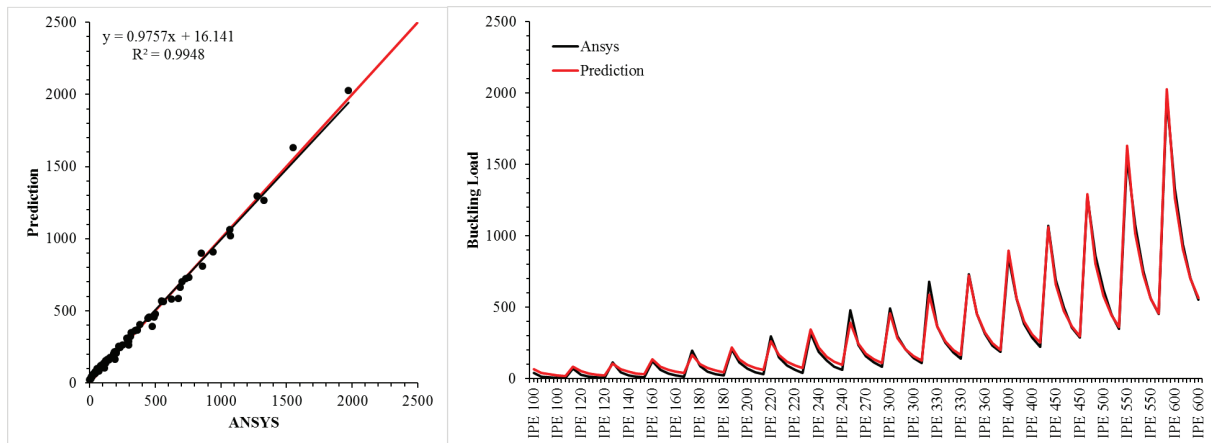| Models	a	b	
Caliber Model1	3.896068277	0.419127105	
	c	d	f
Caliber Model2	0	0.160835288821455	0.919080100568975

Figure 7. Comparisons of the prediction and ANSYS values of the buckling load for Calibration Timoshenko and Gere equation

MAE values of 24. NSE error value was used because of high MSE values. An NSE value greater than 0.9 indicates that the estimate is correct. The scatter plots in Figures 7-8 are quite good as there is no deviation from x=y (45°).

In recent years, machine learning research in the construction industry have used a maximum of 3 performance criteria [47,49,50,52,53,61–65]. The equations created utilizing the six performance criteria have undergone a thorough analysis in this study. Six performance parameters were used to objectively assess the Caliber models' performance.

The correlation coefficient R has been utilized as a performance criterion in machine learning studies in the field of construction the most frequently in recent years [49, 50, 52, 53, 63–67]. The R value for these studies in the literature was discovered to be somewhere in the range of 0.9, and
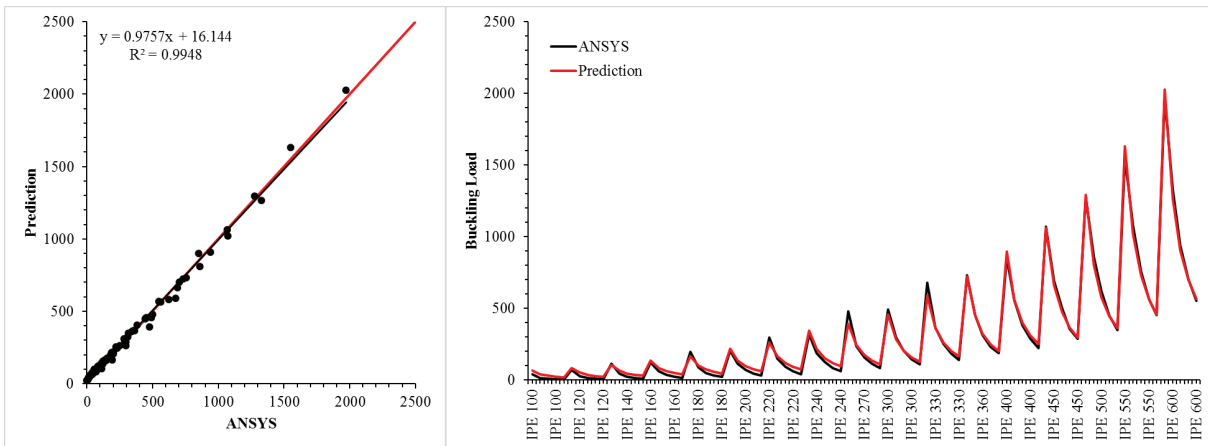
Figure 8. Comparisons of the prediction and ANSYS values of the buckling load for Calibration AISC - DCCPSS

Table 4. Comparison criteria of modified equations

	NSE	MAE	MARE	MSE	RMSE	R2
Caliber Model1	0.994	24.30	51.56	892.56	29.88	0.995
Caliber Model2	0.994	24.29	51.47	891.46	29.86	0.995

the correlation between the actual predicted value and the observed value was only somewhat stronger. Additionally, several researchers used the R^2 criterion to assess the effectiveness of the models they created for machine learning investigations [47,50,53,61]. The R^2 criteria was determined to be more than 0.9 in these investigations. This finding demonstrates that prediction and observation have a stronger link. The determination factor R^2 criteria was utilized in this work instead of the R coefficient, which would have been misleading for assessing the performance of the models. Tables 4 show that the Caliber models' findings meet the R^2 criteria of larger than 0.9 and that there is a stronger connection between prediction and observation.

The amount of time that passed while the suggested strategy was being used is another important finding. It took 0.173 seconds to optimize the coefficients. With the developing technology, the proposed approach for calculating the buckling load is not only accurate but also significantly faster. Thus, decreases the amount of computation necessary to carry out such an analysis.

Excel–Solver has been used in optimization studies in the field of construction in recent years [36,38–40]. However, it was used for the first time in the field of construction in the optimization of the coefficients of an equation in this study.

CONCLUSION

Analytical solutions become very complex when the beam end conditions are a cantilever beam with a fixed support as opposed to a simple support. Therefore, numerical approaches such as the finite element method are needed to solve the fundamental differential equilibrium equations. Despite having various types of smart automating, finite element types, and executed analyses, two identical models examined using the finite element method in two distinct verified software's should have produced findings that are equal. Because the mesh cannot be adjusted, the usage of isoperimetric components on SAP2000 can only be used to make initial estimates for early phases of study. Finite elements with more nodes or integration points are not an option in SAP2000. ANSYS software, which is more suitable for research than design, has been preferred in finite element analysis due to the advantage of the selection and full control of different finite element meshes, where different behaviour rules of materials can be applied, and possible complex analysis applications.

In today's steel specifications, no distinction is made in the design and calculation methods of simply supported beams and cantilever beams under the buckling effect. However, the buckling zones on the steel beams change according to the end support conditions. Considering these situations in differential equilibrium equations creates quite complex problems in generating analytical solutions. Instead, existing analytical formulas were optimized for cantilever beams with reference to finite element analysis. Thanks to the results obtained, the buckling load calculation of cantilever beams can be successfully solved with the help of renewed closed form equations. This renewed

formula can make very high accuracy predictions, which can be an alternative to finite element analysis.

The proposed approach in optimizing the coefficients has taken only 0.173 seconds, it can be concluded that employing Excel-Solver reduces the computational cost that is required to conduct for buckling loads of IPE-Section. 85 numerical calculations were conducted to determine the buckling load of IPE cantilever beams with varied length. Therefore, only cantilever beams with the IPE section are compatible with the calibrated equation created using the Excel-Solver. Other I-section cantilever beams require a significantly wider variety of numerical analysis. In further studies, experimentally validate the proposed method and its results is recommended for buckling load calculations.

NOTATION

P_{cr}	Critical buckling load
L	Beam length
E	Modulus of elasticity
I_y	Moment of inertia about the weak axis
C	Torsional stiffness
C_1	Distortion stiffness
C_b	Moment correction coefficient
F_{cr}	Critical Stress
L_b	Length of element not supported by stability joint
i_{ts}	Effective radius of inertia
J	Torsional constant
C_w	Distortion constant
W_{ex}	Elastic section modulus about the strong axis
h_o	The distance between the centres of gravity of the cross-section flanges
γ_2	a dimensionless coefficient
M_{maks}	The absolute value of the maximum bending moment along the length of the laterally unsupported beam
M_A	The absolute value of the bending moment at 1/4 point of the laterally unsupported beam length.
M_B	The absolute value of the bending moment at 1/2 point of the laterally unsupported beam length.
M_C	The absolute value of the bending moment at 3/4 point of the laterally unsupported beam length.
BL_p	Buckling load estimated by calibrated models
BL_{ansys}	Buckling load obtained from ANSYS analysis
n	Length of the series
BL_{ansys}	Average of the buckling load obtained from ANSYS analysis

DATA AVAILABILITY STATEMENT

The authors confirm that the data that supports the findings of this study are available within the article. Raw data that support the finding of this study are available from the corresponding author, upon reasonable request.

AUTHOR CONTRIBUTION

All authors contributed to the study conception and design. Material preparation, data collection and analysis were performed by Ahmet Özbayrak, Mohammed Kamal Ali and Hatice Çıtakoğlu. The first draft of the manuscript was written by Ahmet Özbayrak, and all authors commented on previous versions of the manuscript. All authors read and approved the final manuscript.

CONFLICT OF INTEREST

On behalf of all authors, the corresponding author states that there is no conflict of interest.

ETHICAL APPROVAL

This article does not contain any studies with human participants or animals performed by any of the authors.

FUNDING DETAILS

No funds, grants, or other support was received.

REFERENCES

[1] Trahair NS. Steel cantilever strength by inelastic lateral buckling. J Constr Steel Res 2010;66:993–999. [CrossRef]

[2] American Institute of Steel Construction. Specification for structural steel buildings. Chicago: American Institute of Steel Construction; 2011.

[3] Turkish Republic - Ministry of Environounment and Urbanization. Çelik yapıların tasarım, hesap ve yapım esaslarına dair yönetmelikte değişiklik yapıl-masına dair yönetmelik. Available at: https://www.resmigazete.gov.tr/eskiler/2018/02/20180215M1-4.htm. Accessed on Jun 12, 2024.

[4] Chen WF, Atsuta T. Theory of beam-columns: Space behavior and design. McGraw-Hill, New York: J. Ross Publishing; 1977.

[5] Chen WF. Structural stability: Theory and implementation. 1st ed. New York: Prentice Hall; 1987.

[6] Timoshenko SP, Gere JM, Prager W. Theory of elastic stability, second edition. J Appl Mech 1962;29:220–221. [CrossRef]

[7] Trahair NS. Inelastic lateral buckling of steel cantilevers. Eng Struct 2020;208:109918. [CrossRef]

[8] ANSYS. ANSYS Help. Release 145 Copyr 2012.

[9] Sapfire. SAP2000 Structural analysis and design. Available at: https://www.csiamerica.com/products/sap2000. Accessed on Jun 26, 2024.

[10] Gonenli C, Das O. Effect of crack location on buckling and dynamic stability in plate frame structures. J Braz Soc Mech Sci Eng 2021;43:311. [CrossRef]

[11] Demirhan AL, Eroğlu HE, Mutlu EO, Yılmaz T, Anil Ö. Experimental and numerical evaluation of inelastic lateral-torsional buckling of I-section cantilevers. J Constr Steel Res 2020;168:105991. [CrossRef]

[12] Samanta A, Kumar A. Distortional buckling in braced-cantilever I-beams. Thin-Walled Struct 2008;46:637–645. [CrossRef]

[13] Ozbasaran H, Aydin R, Dogan M. An alternative design procedure for lateral-torsional buckling of cantilever I-beams. Thin-Walled Struct 2015;90:235–242. [CrossRef]

[14] Ma M, McNatt T, Hays B, Hunter S. Elastic lateral distortional buckling analysis of cantilever I-beams. Ships Offshore Struct 2013;8:261–269. [CrossRef]

[15] Andrade A, e Costa PP, Camotim DRZ. Elastic lateral-torsional buckling of restrained web-tapered I-beams. Comput Struct 2010;88:1179–1196. [CrossRef]

[16] Zhang WF, Liu YC, Hou GL, Chen KS, Ji J, Deng Y, et al. Lateral-torsional buckling analysis of cantilever beam with tip lateral elastic brace under uniform and concentrated load. Int J Steel Struct 2016;16:1161–1173. [CrossRef]

[17] Winatama Kurniawan C, Mahendran M. Elastic lateral buckling of cantilever litesteel beams under transverse loading. Int J Steel Struct 2011;11:395–407. [CrossRef]

[18] Yılmaz T, Kiraç N. Analytical and parametric investigations on lateral torsional buckling of European IPE and IPN beams. Int J Steel Struct 2017;17:695–709. [CrossRef]

[19] Prombut P, Anakpotchanakul C. Deflection of composite cantilever beams with a constant I-cross section. IOP Conf Ser Mater Sci Eng 2019;501:012025. [CrossRef]

[20] Ozbasaran H, Yilmaz T. Shape optimization of tapered I-beams with lateral-torsional buckling, deflection and stress constraints. J Constr Steel Res 2018;143:119–130. [CrossRef]

[21] Rahami H, Kaveh A, Glolipour Y. Sizing, geometry and topology optimization of trusses via force method and genetic algorithm. Eng Struct 2008;30:2360–2369. [CrossRef]

[22] Camp CV, Bichon BJ, Stovali SP. Design of steel frames using ant colony optimization. J Struct Eng 2005;131:369–379. [CrossRef]

[23] Hayalioglu MS, Degertekin SO. Design of non-linear steel frames for stress and displacement constraints with semi-rigid connections via genetic optimization. Struct Multidiscip Optim 2004;27:259–271. [CrossRef]

[24] Lagaros ND, Papadrakakis M. Robust seismic design optimization of steel structures. Struct Multidiscip Optim 2007;33:457–469. [CrossRef]

[25] Lagaros ND, Papadrakakis M. Seismic design of RC structures: A critical assessment in the framework of multi-objective optimization. Earthq Eng Struct Dyn 2007;36:1623–1639. [CrossRef]

[26] Yassami M, Ashtari P. Using fuzzy genetic algorithm for the weight optimization of steel frames with semi-rigid connections. Int J Steel Struct 2014;15:63–73. [CrossRef]

[27] Dehghani S, Fathizadeh SF, Vosoughi AR, Farsangi EN, Yang TY, Hajirasouliha I. Development of a novel cost-effective toggle-brace-curved damper (TBCD) for mid-rise steel structures using multi-objective NSGA II optimization technique. Struct Multidiscip Optim 2020;63:661–688. [CrossRef]

[28] Prendes-Gero MB, Bello-García A, del Coz-Díaz JJ, Suárez-Domínguez FJ, Gero MBP. Optimization of steel structures with one genetic algorithm according to three international building codes. Rev Constr 2018;17:47–59. [CrossRef]

[29] Kaveh A, Moghanni RM, Javadi S. Optimum design of large steel skeletal structures using chaotic firefly optimization algorithm based on the Gaussian map. Struct Multidiscip Optim 2019;60:879–894. [CrossRef]

[30] Perelmuter A, Yurchenko V. Parametric optimization of steel shell towers of high-power wind turbines. Procedia Eng 2013;57:895–905. [CrossRef]

[31] Shaqfa M, Orban Z. Modified parameter-setting-free harmony search (PSFHS) algorithm for optimizing the design of reinforced concrete beams. Struct Multidiscip Optim 2019;60:999–1019. [CrossRef]

[32] Omkar SN, Khandelwal R, Ananth TVS, Naik GN GS. Quantum behaved Particle Swarm Optimization (QPSO) for multi-objective design optimization of composite structures. Expert Syst Appl 2009;36:11312–11322. [CrossRef]

[33] Barraza M, Bojórquez E, Fernández-González E, Reyes-Salazar A. Multi-objective optimization of structural steel buildings under earthquake loads using NSGA-II and PSO. Design Optim Appl Civil Eng 2017;21:488–500. [CrossRef]

[34] Błachut J, Magnucki K. Strength, stability, and optimization of pressure vessels: Review of selected problems. Appl Mech Rev 2008;61:060801. [CrossRef]

[35] Meddaikar YM, Irisarri FX, Abdalla MM. Laminate optimization of blended composite structures using a modified Shepard's method and stacking sequence tables. Struct Multidiscip Optim 2017;55:535–546. [CrossRef]

[36] Cho HK. Optimization of laminated composite cylindrical shells to maximize resistance to buckling and failure when subjected to axial and torsional loads. Int J Precis Eng Manuf 2018;19:85–95. [CrossRef]

[37] Msabawy A Mohammad F. Practical analysis procedures of steel portal frames having different connections rigidities using modified stiffness matrix and end-fixity factor concept. IOP Conf Ser Mater Sci Eng 2019;518:022037. [CrossRef]

[38] Kirsch U. A unified reanalysis approach for structural analysis, design, and optimization. Struct Multidiscip Optim 2003;25:67–85. [CrossRef]

[39] Msabawy A, Mohammad F. Continuous sizing optimization of cold-formed steel portal frames with semi-rigid joints using generalized reduced gradient algorithm. Mater Today Proc 2021;42:2290–2300. [CrossRef]

[40] Taki T. Optimization of flat Z-stiffened panel subjected to compression. Trans Japan Soc Aero Space Sci 2019;62:44−54. [CrossRef]

[41] Vosoughi AR. A developed hybrid method for crack identification of beams. Smart Struct Syst 2015;16:401−414. [CrossRef]

[42] Le LM, Ly H-B, Pham BT, Le VM, Pham TA, Nguyen D-H, et al. Hybrid artificial intelligence approaches for predicting buckling damage of steel columns under axial compression. Materials (Basel) 2019;12:1670. [CrossRef]

[43] Jung ID, Shin DS, Kim D, Lee J, Lee MS, Son HJ, et al. Artificial intelligence for the prediction of tensile properties by using microstructural parameters in high strength steels. Materialia 2020;11:100699. [CrossRef]

[44] Cuong-Le T, Nghia-Nguyen T, Khatir S, Trong-Nguyen P, Mirjalili S, Nguyen KD. An efficient approach for damage identification based on improved machine learning using PSO-SVM. Eng Comput 2022;38:3069−3084. [CrossRef]

[45] Daş O, Bağci Daş D. İzotropik plakaların regressif topluluk öğrenmesi kullanarak serbest titreşim analizi. Eur J Sci Technol 2022:428−434. [CrossRef]

[46] Özbayrak A, Ali MK, Çıtakoğlu H. Buckling load estimation using multiple linear regression analysis and multigene genetic programming method in cantilever beams with transverse stiffeners. Arab J Sci Eng 2023;48:5347−5370. [CrossRef]

[47] Sharifi Y, Tohidi S. Lateral-torsional buckling capacity assessment of web opening steel girders by artificial neural networks - Elastic investigation. Front Struct Civ Eng 2014;8:167−177. [CrossRef]

[48] Onchis DM, Gillich GR. Stable and explainable deep learning damage prediction for prismatic cantilever steel beam. Comput Ind 2021;125:103359. [CrossRef]

[49] Kamane SK, Patil NK, Patagundi BR. Prediction of twisting performance of steel I beam bonded exteriorly with fiber reinforced polymer sheet by using neural network. Mater Today Proc 2021;43:514−519. [CrossRef]

[50] Nguyen TA, Ly HB, Tran VQ. Investigation of ANN architecture for predicting load-carrying capacity of castellated steel beams 2021;6697923. [CrossRef]

[51] Limbachiya V, Shamass R. Application of artificial neural networks for web-post shear resistance of cellular steel beams. Thin Walled Struct 2021;161:107414. [CrossRef]

[52] Hosseinpour M, Rossi A, de Souza ASC, Sharifi Y. New predictive equations for LDB strength assessment of steel-concrete composite beams. Eng Struct 2022;258:114121. [CrossRef]

[53] Mohanty N, Sasmal SK, Uttam, Mishra UK, Sahu SK. Experimental and computational analysis of free in-plane vibration of curved beams. J Vib Eng Technol 2022;11:1777−1796. [CrossRef]

[54] Neves M, Basaglia C, Camotim D. Stiffening optimisation of conventional cold-formed steel cross-sections based on a multi-objective Genetic Algorithm and using Generalised Beam Theory. Thin Walled Struct 2022;179:109713. [CrossRef]

[55] Galéa Y.) LTBeam Version 1.0. 11. CTICM Fr 2012.

[56] Access Steel. NCCI: Elastic critical moment for lateral torsional buckling. Available at: https://www.steelconstruction.info/images/0/0f/SN003b.pdf. Accessed Jun 26, 2024.

[57] ECCS. Rules for Member Stability in EN 1993-1-1: Background documentation and design guidelines. Available at: https://store.steelconstruct.com/site/index.php?module=store&target=publicStore&id_category=13&id=19. Accessed Jun 26, 2024.

[58] Karunanithi N, Grenney WJ, Whitley D, Bovee K. Neural networks for river flow prediction. J Comput Civ Eng 1994;8:201−220. [CrossRef]

[59] Citakoglu H. Comparison of artificial intelligence techniques for prediction of soil temperatures in Turkey. Theor Appl Climatol 2017;130:545−556. [CrossRef]

[60] Nash JE, Sutcliffe JV. River flow forecasting through conceptual models part I - A discussion of principles. J Hydrol 1970;10:282−290. [CrossRef]

[61] Graciano C, Kurtoglu AE, Casanova E. Machine learning approach for predicting the patch load resistance of slender austenitic stainless steel girders. Structures 2021;30:198−205. [CrossRef]

[62] Ferreira FPV, Shamass R, Limbachiya V, Tsavdaridis KD, Martins CH. Lateral-torsional buckling resistance prediction model for steel cellular beams generated by Artificial Neural Networks (ANN). Thin Walled Struct 2022;170:108592. [CrossRef]

[63] Sharifi Y, Moghbeli A, Hosseinpour M, Sharifi H. Neural networks for lateral torsional buckling strength assessment of cellular steel I-beams. 2019;22:2192−2202. [CrossRef]

[64] Abambres M, Rajana K, Tsavdaridis KD, Ribeiro TP. Neural network-based formula for the buckling load prediction of I-section cellular steel beams. Computers 2019;8:2. [CrossRef]

[65] Moghbeli A, Sharifi Y. New predictive equations for lateral-distortional buckling capacity assessment of cellular steel beams. Structures 2021;29:911−923. [CrossRef]

[66] Hosseinpour M, Moghbeli A, Sharifi Y. Evaluation of lateral-distortional buckling strength of castellated steel beams using regression models. Innov Infrastruct Solut 2021;6:142. [CrossRef]